

# Finite-Size Scaling for Directed Percolation Models

Santanu Sinha and S. B. Santra

*Department of Physics, Indian Institute of Technology*

*Guwahati, Guwahati-781039, Assam, India*

## Abstract

A simple finite-size scaling theory is proposed here for anisotropic percolation models considering the cluster size distribution function as generalized homogeneous function of the system size and two connectivity lengths. The proposed scaling theory has been verified numerically on two different anisotropic percolation models.

## I. INTRODUCTION

Percolation, a model of disorder[1], shows a geometrical phase transition at the percolation threshold characterized by singularities of cluster related quantities similar to the critical phenomena or second order phase transition in thermodynamic systems[2]. The singularities occurred in phase transitions are generally described by power laws characterized by well defined critical exponents. The set of critical exponents and the scaling relations among them characterize the universality class of a system. Since most systems are not solvable analytically, numerical methods are employed in order to investigate the critical behavior. At the same time, the numerical results are very often limited by the finite system size. In a finite system, there is rounding and shifting of critical singularities depending on the ratio of correlation length  $\xi$  to the linear dimension  $L$  of the system. In order to obtain the behavior of the infinite systems, the results of finite systems are generally extrapolated using finite-size scaling (FSS)[3]. However, there are very few FSS theory for anisotropic models of statistical physics[3, 4]. FSS theory is available for isotropic percolation models such as ordinary percolation[5] and spiral percolation (percolation under rotational constraint)[6]. Anisotropic percolation clusters are generated if an external space fixed directional constraint is applied on the percolation model. Such models are directed percolation (DP)[7] and directed spiral percolation (DSP)[8]. In these models, there are two connectivity lengths  $\xi_{\parallel}$  and  $\xi_{\perp}$  and they become singular at the percolation threshold with two different critical exponents. Considering DP as a minimal stochastic Markovian process represented by Langevin equation, a FSS theory has been developed by Janssen *et al*[9] below the upper critical dimension  $d_c = 4$  and above  $d_c$  by Lübeck and Janssen[10]. Usually, the anisotropy considered in the FSS theory is either in the interaction between the constituent particles[4] or in the topology of the system (strip like structure)[3]. However, in a geometrical model like percolation, the particles are simply occupied with a probability  $p$  in absence of any interaction between them. The models are generally defined on topologically isotropic systems of size  $L \times L$ . For such noninteracting anisotropic models defined on topologically isotropic systems, a simple phenomenological FSS theory is proposed here. The proposed FSS theory for anisotropic percolation models is developed here considering the cluster size distribution function as a generalized homogeneous function[2] of occupation probability  $p$  and ratios of connectivity lengths with the system size.

## II. ANISOTROPIC PERCOLATION MODELS

There are two well known anisotropic percolation models DP[7] and DSP[8]. In DP, a directional field  $E$  is present in the model. The direction of applied  $E$  field from upper left to the lower right corner of the lattice is considered here. As an effect of the  $E$  field, the empty sites to the right and to the bottom of an occupied site are only eligible for occupation. The eligible sites are then occupied with probability  $p$ . Accordingly, the clusters grow in the diagonal direction along  $E$ . In the case of DSP, a crossed rotational field  $B$  is also present in addition to the directional field  $E$ . In this problem,  $E$  field is applied from left to right in the plane of the lattice and  $B$  is applied perpendicular to  $E$  and into the plane of the lattice (viewed from top). Due to  $E$  field, empty site on the right of an occupied site is eligible for occupation whereas for  $B$  field, empty sites in the forward and clockwise rotational directions are eligible for occupation. The forward direction is the direction from which the present site is occupied. Because of the simultaneous presence of both the  $E$  and  $B$  fields crossed to each other, a Hall field appears in the system perpendicular to both  $E$  and  $B$ . As a result, an effective directional constraint  $E_{\text{eff}}$  acts on the system along the left upper to right lower diagonal of the lattice. The clusters grow along the effective field  $E_{\text{eff}}$ [8]. A cluster is considered to be a spanning cluster, if either the lateral or the vertical extension of a cluster becomes equal to the dimension of the lattice  $L$ . At the percolation threshold  $p_c$ , a spanning cluster appears for the first time in a system. It was found as  $p_c \approx 0.705489$  for DP[7] and  $p_c \approx 0.6550$  for DSP[8] on the square lattice in case of site occupation. For a given finite system  $L$ , the cluster properties are calculated generating finite clusters.

Typical large clusters for DP and DSP generated on  $256 \times 256$  square lattice at their respective percolation thresholds are shown in Fig.1. It can be seen that the clusters are anisotropic and rarefied. In order to characterize the cluster's connectivity property, two length scales  $\xi_{\parallel}$  and  $\xi_{\perp}$  are required.  $\xi_{\parallel}$  is the extension along the elongation of the cluster and  $\xi_{\perp}$  is the extension in the perpendicular direction of the elongation. Two connectivity lengths  $\xi_{\parallel}$  and  $\xi_{\perp}$  diverge with different critical exponents  $\nu_{\parallel}$  and  $\nu_{\perp}$  at the  $p = p_c$ . Though the DSP cluster grows along an effective directional constraint  $E_{\text{eff}}$ , the critical properties of the clusters at  $p = p_c$  were found different from that of DP clusters. Accordingly DP and DSP belong to two different universality classes[8].

### III. FSS THEORY

A system is said to be finite if the system size  $L < \xi$ , the connectivity length. In the case of anisotropic percolation models, there are two connectivity lengths  $\xi_{\parallel}$  and  $\xi_{\perp}$  where  $\xi_{\parallel}$  always greater than  $\xi_{\perp}$ . The finiteness of the system size then can be defined in terms of  $\xi_{\parallel}$ . According to the theory of critical phenomena, thermodynamic functions become generalized homogeneous functions at the critical point[2]. The cluster size distribution function  $P_s(p, L)$  describing the geometrical quantities here in percolation is then expected to be a generalized homogeneous function at the percolation threshold  $p_c$ . A simple phenomenological FSS theory for these anisotropic percolation models is proposed here assuming  $P_s(p, L)$  as a generalized homogeneous function. In order to develop FSS theory, the scaling of the order parameter of the percolation transition  $P_{\infty}$ , probability to find a site in a spanning cluster, with the system size  $L$  is considered first. At the end, the scaling form will be generalized for arbitrary cluster related quantity  $Q$ .

In the case of an infinite system, the order parameter  $P_{\infty}$  becomes singular at  $p = p_c$  as

$$P_{\infty} \sim (p - p_c)^{\beta} \quad (1)$$

with a critical exponent  $\beta$ . In a finite geometry with topologically symmetric dimension  $L \times L$ , the critical singularity of  $P_{\infty}$  for anisotropic percolation clusters depends not only on  $(p - p_c)$  but also on the ratios  $\xi_{\parallel}/L$  and  $\xi_{\perp}/L$ . The functional dependence of  $P_{\infty}$  on these parameters is then given by

$$P_{\infty}(L, p) = \mathcal{F}[(p - p_c), \frac{\xi_{\parallel}}{L}, \frac{\xi_{\perp}}{L}]. \quad (2)$$

For an infinite system, at  $p = p_c$ ,  $\xi_{\parallel}$  is infinitely large and the system properties become independent of the system size  $L$ . Accordingly, two parameters  $\xi_{\parallel}/L$  and  $\xi_{\perp}/L$  in  $P_{\infty}$  given in Eq.2 can be reduced to a single parameter  $\xi_{\parallel}/\xi_{\perp}$ . Thus,  $P_{\infty}$  in Eq.2 can be expressed as

$$P_{\infty} = \mathcal{G}[(p - p_c), \xi_{\parallel}/\xi_{\perp}]. \quad (3)$$

It is now important to know how  $\xi_{\parallel}$  and  $\xi_{\perp}$  scale with the dimension  $L$  of the finite system at the percolation threshold  $p_c$ . Two new scaling forms for  $\xi_{\parallel}$  and  $\xi_{\perp}$  with  $L$  are assumed as,

$$\xi_{\parallel} \approx L^{\theta_{\parallel}} \quad \text{and} \quad \xi_{\perp} \approx L^{\theta_{\perp}} \quad (4)$$

where  $\theta_{\parallel}$  and  $\theta_{\perp}$  are two new exponents. It is now possible to define  $P_{\infty}$  in terms of the system size  $L$  as

$$P_{\infty} = F[(p - p_c), L^{\theta_{\parallel} - \theta_{\perp}}]. \quad (5)$$

Assuming the order parameter  $P_{\infty}$  as a generalized homogeneous function of  $(p - p_c)$  and  $L^{\theta_{\parallel} - \theta_{\perp}}$ , it is possible to express  $P_{\infty}$  as

$$F[\lambda^a(p - p_c), \lambda^b L^{\theta_{\parallel} - \theta_{\perp}}] = \lambda P_{\infty} \quad (6)$$

where  $a$  and  $b$  are arbitrary numbers and  $\lambda$  is a parameter. The above relation is valid for any value of  $\lambda$ . For  $\lambda = L^{-(\theta_{\parallel} - \theta_{\perp})/b}$ ,  $P_{\infty}$  takes the form

$$P_{\infty} = L^{A(\theta_{\parallel} - \theta_{\perp})} F[(p - p_c) L^{-B(\theta_{\parallel} - \theta_{\perp})}, 1] \quad (7)$$

where  $A = 1/b$  and  $B = a/b$  are two exponents to be determined. However, as  $L \rightarrow \infty$ , the  $L$  dependence of  $P_{\infty}$  will vanish. Therefore,  $F[z]$  should go as  $z^{A/B}$  in the limit  $L \rightarrow \infty$  when  $z = (p - p_c) L^{-B(\theta_{\parallel} - \theta_{\perp})}$ . In that case,

$$\begin{aligned} P_{\infty} &\approx L^{A(\theta_{\parallel} - \theta_{\perp})} \left( L^{-B(\theta_{\parallel} - \theta_{\perp})} (p - p_c) \right)^{A/B} \\ &\approx (p - p_c)^{A/B}. \end{aligned} \quad (8)$$

The order parameter exponent  $\beta$  is then given by  $\beta = A/B$ .

The size of a cluster is given by the number of occupied sites  $s$  in that cluster. For anisotropic clusters, there are two connectivity lengths which could be measured in terms of radii of gyration  $R_{\parallel}$  and  $R_{\perp}$  with respect to two principal axes of the cluster. The size of the cluster can also be calculated in terms of area defined by  $R_{\parallel}$  and  $R_{\perp}$ . It is expected that the cluster size should scale as  $s \approx R_{\parallel} R_{\perp}^{(d_f - 1)}$  at  $p = p_c$  and it should go as  $s \approx R_{\parallel} R_{\perp}^{(d - 1)}$  above  $p_c$  where  $d$  is the spatial dimension of the lattice and  $d_f$  is the fractal dimension of the infinite clusters generated on the same lattice. The percolation probability  $P_{\infty}$  is the ratio of the number of sites on the infinite cluster to the total number of sites and can be given as

$$P_{\infty} = \frac{R_{\parallel} R_{\perp}^{(d_f - 1)}}{R_{\parallel} R_{\perp}^{(d - 1)}} = R_{\perp}^{(d_f - d)}. \quad (9)$$

Assuming  $R_{\perp} \approx \xi_{\perp} \approx L^{\theta_{\perp}}$  at  $p_c$ , Eq.9 leads to  $P_{\infty} \sim L^{\theta_{\perp}(d_f - d)}$ . Also at  $p = p_c$ , the functional form of  $P_{\infty}$ , given in Eq.7, reduces to  $P_{\infty} \sim L^{A(\theta_{\parallel} - \theta_{\perp})}$ . Therefore, exponent  $A$

can be obtained in terms of the new exponents  $\theta_{\parallel}$  and  $\theta_{\perp}$  as

$$A = \frac{\theta_{\perp}(d_f - d)}{\theta_{\parallel} - \theta_{\perp}}. \quad (10)$$

Inserting the value of  $A$  in Eq.7 at  $p = p_c$  it reduces to

$$P_{\infty} = L^{\theta_{\perp}(d_f - d)} F[0] = \xi_{\perp}^{(d_f - d)} F[0] = \xi_{\parallel}^{(d_f - d)\theta_{\perp}/\theta_{\parallel}} F[0] \quad (11)$$

where  $F[0]$  is a constant. For an infinite system, at  $p = p_c$ , the connectivity lengths diverge as

$$\xi_{\parallel} \sim |p - p_c|^{-\nu_{\parallel}} \quad \xi_{\perp} \sim |p - p_c|^{-\nu_{\perp}} \quad (12)$$

where  $\nu_{\parallel}$  and  $\nu_{\perp}$  are connectivity exponents. The following scaling relations then can easily be extracted as

$$\beta = \nu_{\perp}(d - d_f) \quad \text{and} \quad \beta = \nu_{\parallel}(d - d_f)\theta_{\perp}/\theta_{\parallel}. \quad (13)$$

The first one of these relations is the hyperscaling relation[1] and the second one is a new scaling relation connecting the exponents  $\theta_{\perp}$  and  $\theta_{\parallel}$ . Using the above scaling relations and eliminating  $(d - d_f)$ , the values of the exponents  $A$  and  $B$  can be obtained as

$$\begin{aligned} A &= -\frac{\theta_{\perp}\beta}{(\theta_{\parallel} - \theta_{\perp})\nu_{\perp}} = -\frac{\theta_{\parallel}\beta}{(\theta_{\parallel} - \theta_{\perp})\nu_{\parallel}} \\ B &= -\frac{\theta_{\perp}}{(\theta_{\parallel} - \theta_{\perp})\nu_{\perp}} = -\frac{\theta_{\parallel}}{(\theta_{\parallel} - \theta_{\perp})\nu_{\parallel}}. \end{aligned} \quad (14)$$

From the expressions of  $A$  and  $B$ , it can be seen that  $\nu_{\parallel}/\theta_{\parallel} = \nu_{\perp}/\theta_{\perp}$ . This is consistent with the assumption  $\xi_{\perp} \sim \xi_{\parallel}^{\theta_{\parallel}/\theta_{\perp}}$  in Eq.4 and the fact  $\xi_{\perp} \sim \xi_{\parallel}^{\nu_{\parallel}/\nu_{\perp}}$  for an infinite system. Consequently, one can define the anisotropy exponent

$$\theta = \theta_{\parallel}/\theta_{\perp} = \nu_{\parallel}/\nu_{\perp} \quad (15)$$

as suggested in Ref.[12]. This is interesting to note that this equation is always valid even if the hyperscaling relations are not exactly satisfied. It is known that hyperscaling relations are not satisfied in case of DP[13].

Since the values of  $A$  and  $B$  are now known, the finite-size scaling form of  $P_{\infty}$  can be given as

$$P_{\infty}(L, p) = L^{-\beta\theta_{\parallel}/\nu_{\parallel}} F[(p - p_c)L^{\theta_{\parallel}/\nu_{\parallel}}] = L^{-\beta\theta_{\perp}/\nu_{\perp}} F[(p - p_c)L^{\theta_{\perp}/\nu_{\perp}}]. \quad (16)$$

It is interesting to note that a finite size scaling relation is obtained in terms of two unknown exponents  $\theta_{\parallel}$ ,  $\theta_{\perp}$  and two known exponents  $\nu_{\parallel}$ ,  $\nu_{\perp}$ .

Now, the finite size scaling form of the order parameter  $P_{\infty}$  can be generalized for any cluster related quantity  $Q$ . Suppose that in an infinite system, as  $p \rightarrow p_c$  the cluster related quantity  $Q$  scales as

$$Q \sim |p - p_c|^{-q} \quad (17)$$

where  $q$  is a critical exponent. In a finite geometry, it is then expected that the cluster related quantities in general will obey the finite size scaling law given by

$$Q(L, p) = L^{q\theta_{\parallel}/\nu_{\parallel}} F[(p - p_c)L^{\theta_{\parallel}/\nu_{\parallel}}] = L^{q\theta_{\perp}/\nu_{\perp}} F[(p - p_c)L^{\theta_{\perp}/\nu_{\perp}}]. \quad (18)$$

It should be mentioned here that the finite size scaling obtained here for the anisotropic cluster is very similar to that of isotropic clusters. In isotropic FSS,  $Q(L, p) = L^{q/\nu} F[(p - p_c)L^{1/\nu}]$  where  $\nu$  is the connectivity length exponent[5]. In Eq.18,  $1/\nu$  is replaced by  $\theta_{\parallel}/\nu_{\parallel}$  or  $\theta_{\perp}/\nu_{\perp}$  since it is assumed that the connectivity lengths  $\xi_{\parallel}$  and  $\xi_{\perp}$  scale with the system size  $L$  with exponents  $\theta_{\parallel}$  and  $\theta_{\perp}$ . However, it should be noticed that the FSS relation with respect to  $\xi_{\perp}$ , the transverse length, is new and nontrivial.

The exponents  $\theta_{\parallel}$  and  $\theta_{\perp}$  are measured below for both DP and DSP clusters and the FSS theory developed here is applied to the cluster related quantities of both the models.

#### IV. VERIFICATION OF FSS THEORY

In order to verify the proposed FSS theory, simulations are performed on the square lattice of sizes  $L = 128$  to 2048 in multiple of 2. Average has been taken over  $5 \times 10^4$  large finite clusters. First, the exponents  $\theta_{\parallel}$  and  $\theta_{\perp}$  which describes the dependence of connectivity lengths with the system size  $L$  are determined. Since, clusters are grown following single cluster growth algorithm, the connectivity lengths are given by  $\xi_{\parallel}^2 = 2 \sum'_s R_{\parallel}^2 s P_s(p, L) / \sum'_s s P_s(p, L)$  and  $\xi_{\perp}^2 = 2 \sum'_s R_{\perp}^2 s P_s(p, L) / \sum'_s s P_s(p, L)$  where  $R_{\parallel}$  and  $R_{\perp}$  are radii of gyration with respect to two principal axes of the cluster.  $R_{\parallel}$  and  $R_{\perp}$  are estimated from the eigenvalues of the moment of inertia tensor, a  $2 \times 2$  matrix here. The cluster size distribution function  $P_s(p, L)$  is defined as  $N_s/N_{tot}$  where  $N_s$  is the number of  $s$ -sited clusters out of  $N_{tot}$  clusters generated on a given system size.  $\xi_{\parallel}$  and  $\xi_{\perp}$  are measured for various system sizes  $L$  at  $p = p_c$  for both DP and DSP clusters and plotted against the system size  $L$  in Fig.2(a) and Fig.2(b)

respectively. The squares represent the data of DP and the circles represent that of DSP. There are two things to notice. First, the exponent  $\theta_{\parallel}$  is found  $\approx 1$  for both the models. It is expected. Because, for the given field configuration the clusters are elongated along the diagonal of the lattice and  $\xi_{\parallel}$ , extension along the elongation of the cluster, then should be  $\approx \sqrt{2}L$  for large clusters. Second, the exponent  $\theta_{\perp}$  is found different for DP and DSP:  $\theta_{\perp} \approx 0.64 \pm 0.01$  for DP and  $\theta_{\perp} \approx 0.83 \pm 0.01$  DSP. Assuming  $\theta_{\parallel} = 1$ , one should have  $\theta_{\perp} = \nu_{\perp}/\nu_{\parallel}$ . Since for DP,  $\nu_{\perp} = 1.0972 \pm 0.0006$  and  $\nu_{\parallel} = 1.7334 \pm 0.001$  the expected value of  $\theta_{\perp}$  is  $\approx 0.633$ . Similarly for DSP, the expected value of  $\theta_{\perp}$  is  $\approx 0.84$  since  $\nu_{\perp} = 1.12 \pm 0.03$  and  $\nu_{\parallel} = 1.33 \pm 0.01$ . The measured values are close to the expected values for both DP and DSP. This implies that the system properties scale with the system size  $L$  at  $p = p_c$  in the similar manner as it behaves with  $p$  around  $p_c$  for a given large system size. It can also be noticed that the magnitude of  $\xi_{\perp}$  is different for DP and DSP.  $\xi_{\perp}$  is larger for the DSP clusters in comparison to that of DP clusters whereas  $\xi_{\parallel}$  of DSP clusters is slightly smaller than that of DP clusters. Consequently the DSP clusters are less anisotropic than DP clusters.

Next, the average cluster size  $\chi$  is measured for different system size  $L$  at  $p = p_c$ . In single cluster growth algorithm, the average cluster size is defined as  $\chi = \sum'_s s P_s(p, L)$ , where  $P_s(p, L)$  is the cluster size distribution function. In an infinite system,  $\chi$  diverges as:  $\chi \sim |p - p_c|^{-\gamma}$ ,  $\gamma$  is a critical exponent. According to the FSS theory, it should behave as  $\chi(L) \sim L^{\gamma\theta_{\parallel}/\nu_{\parallel}}$  or  $\chi(L) \sim L^{\gamma\theta_{\perp}/\nu_{\perp}}$  at  $p = p_c$ . In Fig.3, the average cluster size  $\chi$  is plotted against the system size  $L$  for both DP and DSP. The cluster size  $\chi$  follows a power law with the system size  $L$ . The obtained slopes are  $1.31 \pm 0.01$  for DP and  $1.38 \pm 0.01$  for DSP. The expected values of the ratio of the exponents are  $\gamma/\nu_{\parallel} \approx 1.31$  and  $\gamma\theta_{\perp}/\nu_{\perp} \approx 1.33$  for DP where  $\gamma = 2.2772 \pm 0.0003$ . For DSP  $\gamma = 1.85 \pm 0.01$  and the expected ratios of the exponents are:  $\gamma/\nu_{\parallel} \approx 1.39$  and  $\gamma\theta_{\perp}/\nu_{\perp} \approx 1.37$ . It can be seen that the measured values are in agreement with that of the expected values within error bars. It confirms that the cluster properties follow the proposed finite size scaling theory. It is not surprising that the scaling theory works with  $\xi_{\parallel}$ . However, the proposed theory works with  $\xi_{\perp}$ , the transverse length. This is a new result.

Finally, the FSS function form has been verified. The average cluster size is given as  $\chi(L, p) = L^{\gamma\theta_{\parallel}/\nu_{\parallel}} F[(p - p_c)L^{\theta_{\parallel}/\nu_{\parallel}}] = L^{\gamma\theta_{\perp}/\nu_{\perp}} F[(p - p_c)L^{\theta_{\perp}/\nu_{\perp}}]$  for different system size  $L$ . In Fig.4, the scaled average size  $\chi/L^{\gamma\theta_{\parallel}/\nu_{\parallel}}$  is plotted against the scaled variable  $z = (p -$



$p_c)L^{\theta_{\parallel}/\nu_{\parallel}}$ . A reasonable data collapse is obtained for both DP and DSP. In the inset of Fig.4, the data collapse is shown by plotting  $\chi/L^{\theta_{\perp}/\nu_{\perp}}$  versus  $z = (p - p_c)L^{\theta_{\perp}/\nu_{\perp}}$ . It can be seen that the tail of the scaling function  $F(z)$  shows a power law behavior in both the models with two different scaling exponents, approximately 2.23 for DP and 1.86 for DSP. Once again it confirms that DP and DSP follow anisotropic finite size scaling and belong to two different universality classes. Note that, these exponents are close to the respective cluster size critical exponents  $\gamma$  for infinite systems as expected.

## V. CONCLUSION

A finite size scaling theory is proposed here for anisotropic percolation models like DP and DSP. In this theory the cluster size distribution is assumed to be a generalized homogeneous function of the  $(p - p_c)$  and the ratios of the connectivity lengths  $\xi_{\parallel}$  and  $\xi_{\perp}$  to the system size  $L$ . Reducing the functional dependence from three variables to two variables  $(p - p_c)$  and  $\xi_{\parallel}/\xi_{\perp}$  and assuming a new scaling form of  $\xi_{\parallel}$  and  $\xi_{\perp}$  with the system size  $L$ , a finite size scaling form of the cluster properties are obtained. Following a single cluster growth Monte Carlo algorithm, clusters are generated at the percolation threshold for DP and DSP varying the system size  $L$ . The numerical simulation confirms the proposed scaling relations as well as the scaling function form. It could be considered as a simplest possible anisotropic finite size scaling theory for directed percolation models.

**Acknowledgment:** SS thanks CSIR, India for financial support.

- 
- [1] A. Bunde and S. Havlin, in *Fractals and Disordered Systems*, edited by A. Bunde and S. Havlin (Springer-Verlag, Berlin, 1991); K. Christensen and N. R. Moloney, *Complexity and Criticality*, (World Scientific, London, 2005).
  - [2] H. E. Stanley, *Introduction to Phase Transitions and Critical Phenomena*, (Oxford University Press, New York, 1987); J. M. Yeomans, *Statistical Mechanics of Phase Transitions*, (Oxford University Press, New York, 1994).
  - [3] M. N. Barber, in *Phase Transitions and Critical Phenomena*, Vol. 8, edited by C. Domb and J. L. Lebowitz (Academic Press, New York, 1984); J. L. Cardy, *Finite-size Scaling*, edited by

- J. L. Cardy (North Holland, Amsterdam, 1988).
- [4] K. Binder and J. S. Wang, *J. Stat. Phys.* **55**, 87 (1989); A. M. Szpilka and V. Privman, *Phys. Rev. B* **28**, 6613 (1983).
- [5] D. Stauffer and A. Aharony, *Introduction to Percolation Theory*, 2nd edition, (Taylor and Francis, London, 1994).
- [6] S. B. Santra and I. Bose, *J. Phys. A* **24**, 2367 (1991) and references there in.
- [7] H. Hinrichsen, *Adv. Phys.* **49**, 815 (2000) and references there in.
- [8] S. B. Santra, *Eur. Phys. J. B* **33**, 75 (2003); S. Sinha and S. B. Santra, *Eur. Phys. J. B.* **39**, 513 (2004); S. Sinha and S. B. Santra, *Int. J. Mod. Phys. C* **16**, 1251 (2005).
- [9] H. K. Janssen, B. Schaub and B. Schmittmann, *Z. Phys. B: Condens. Matter* **71**, 377 (1988).
- [10] S. Lübeck and H. K. Janssen, *Phys. Rev. E* **72**, 016119 (2005).
- [11] J. W. Essam, K. De'Bell, J. Adler and F. M. Bhatti, *Phys. Rev. B* **33**, 1982 (1986); J. W. Essam, A. J. Guttmann and K. De'Bell, *J. Phys. A: Math. Gen.* **21**, 3815 (1988).
- [12] W. Kinzel and J. M. Yeomans, *J. Phys. A: Math. Gen.* **14**, L163 (1981); J. K. Williams and N. D. Mackenzie, *J. Phys. A: Math. Gen.* **17**, 3343 (1984).
- [13] M. Henkel and V. Privman, *Phys. Rev. Lett.* **65**, 1777 (1990).

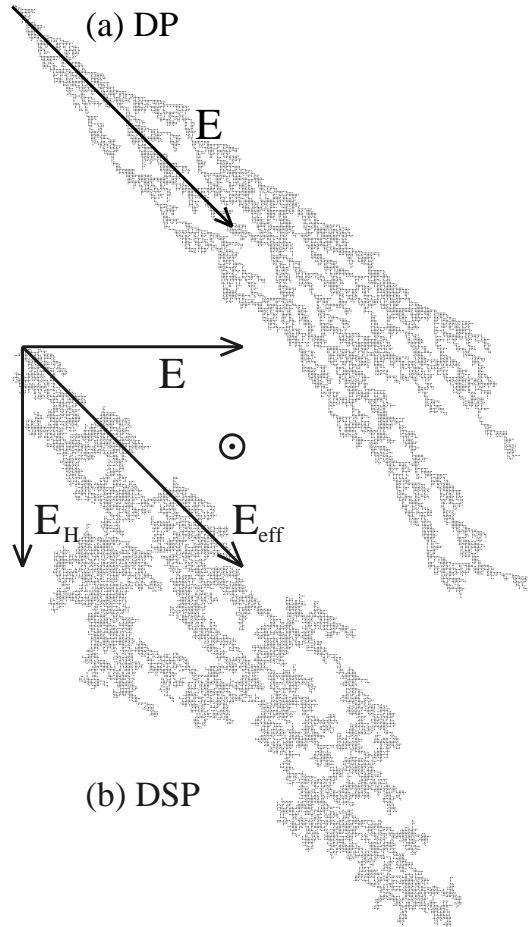


FIG. 1: Typical large clusters of (a) directed percolation and (b) directed spiral percolation generated at  $p = p_c$  on a square lattice of size  $L = 256$ . Arrows represent the directional field  $E$  and the encircled dot represents the rotational field  $B$ .

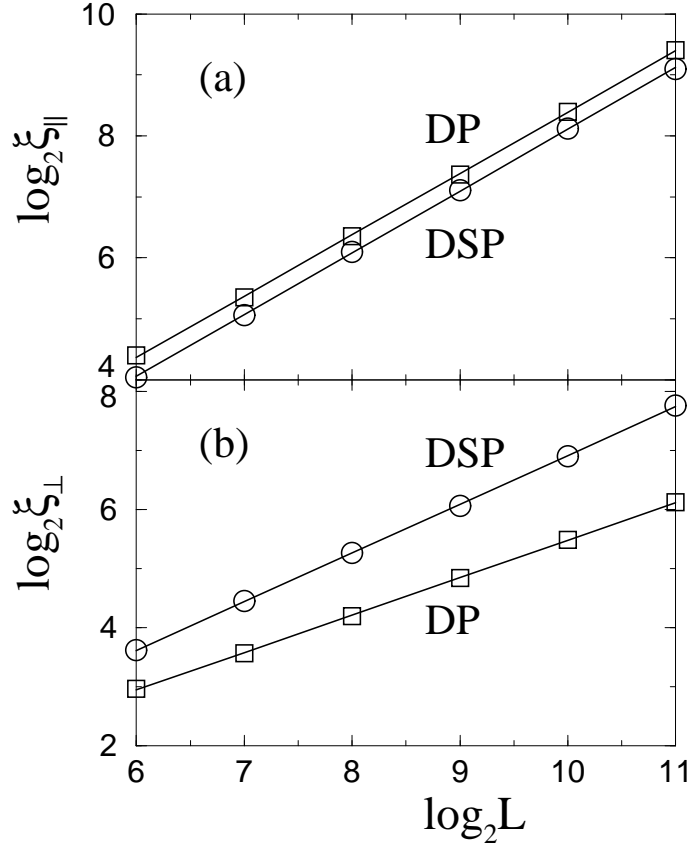


FIG. 2: Plot of (a)  $\xi_{\parallel}$  versus system size  $L$  and (b)  $\xi_{\perp}$  versus  $L$  for the DP ( $\square$ ) and DSP ( $\circ$ ) clusters at their respective percolation thresholds. From the slopes, values of  $\theta_{\parallel}$  and  $\theta_{\perp}$  are obtained as  $\theta_{\parallel} = 1.01 \pm 0.01$  and  $\theta_{\perp} = 0.64 \pm 0.01$  for DP clusters. For DSP, the values are  $\theta_{\parallel} = 1.01 \pm 0.01$  and  $\theta_{\perp} = 0.83 \pm 0.01$  respectively.

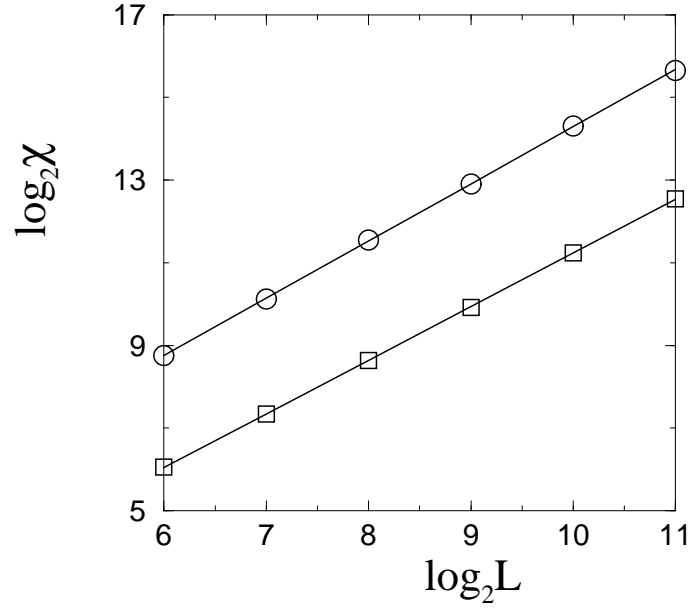


FIG. 3: Plot of average cluster size  $\chi$  versus system size  $L$  for the DP ( $\square$ ) and DSP ( $\circ$ ) clusters at  $p_c$ . From the slopes, the ratio of  $\gamma_{\theta_{\parallel}}/\nu_{\parallel}$  or  $\gamma_{\theta_{\perp}}/\nu_{\perp}$  is obtained as  $1.31 \pm 0.01$  and  $1.38 \pm 0.01$  for DP and DSP respectively.

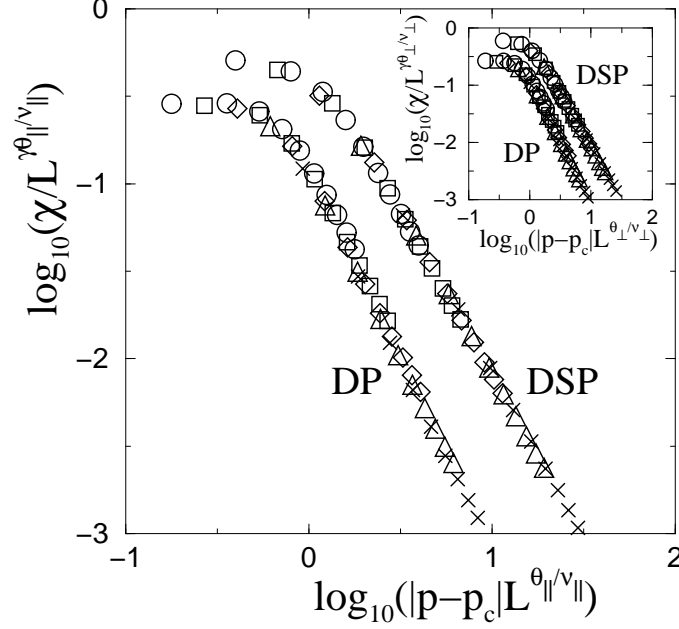


FIG. 4: Plot of scaled average cluster size  $\chi(p, L)/L^{\gamma_{\theta_{\parallel}}/\nu_{\parallel}}$  versus scaled variable  $|p - p_c|L^{\theta_{\parallel}/\nu_{\parallel}}$  for DP and DSP clusters for different values of  $L$  and  $p$ . The data plotted correspond to different system sizes of  $L = 128$  ( $\circ$ ),  $256$  ( $\square$ ),  $512$  ( $\diamond$ ),  $1024$  ( $\triangle$ ) and  $2048$  ( $\times$ ). The  $|p - p_c|$  values here are 0.01 to 0.10 in the interval of 0.01. In the inset, the data collapse is shown plotting  $\chi(p, L)/L^{\gamma_{\theta_{\perp}}/\nu_{\perp}}$  versus  $|p - p_c|L^{\theta_{\perp}/\nu_{\perp}}$ .